

# Nanosized rhodium oxide particles in the MCM-41 mesoporous molecular sieve

Ravichandra S. Mulukutla,<sup>a</sup> Kiyotaka Asakura,<sup>b</sup> Seitaro Namba<sup>c</sup> and Yasuhiro Iwasawa<sup>\*a†</sup>

<sup>a</sup> Department of Chemistry, Graduate School of Science, The University of Tokyo, Hongo, Bunkyo-Ku, Tokyo 113-0033, Japan

<sup>b</sup> Research Center for Spectrochemistry, Graduate School of Science, The University of Tokyo, Hongo, Bunkyo-Ku, Tokyo 113-0033, Japan

<sup>c</sup> Department of Materials, Teikyo University of Science and Technology, Uenohara-machi, Kitatsuru-gun, Yamanashi 409-0193, Japan

## Nanosized rhodium oxide-containing MCM-41 (Rh-MCM-41) mesoporous molecular sieves are synthesized and characterized by XRD, TEM, N<sub>2</sub> adsorption, NMR, XPS and EXAFS.

The discovery<sup>1,2</sup> of the novel mesoporous silicate based MCM-41 molecular sieve has generated much interest to design hybrid atom-containing MCM-41 by isomorphous substitution of transition metals into the framework or by functionalisation of the silanols in the pore channels for their applications to catalysis and advanced materials.<sup>3–5</sup> Noble metals such as Pt,<sup>6,7</sup> Pd,<sup>8,9</sup> and Ru<sup>10</sup> were supported on MCM-41, and Ag/Ru bimetallic nanoparticles<sup>11</sup> were supported inside the MCM-41 channels and found to be active compared with the corresponding conventional supported catalysts. However there is no study related to the synthesis of noble metal-containing MCM-41 by addition of noble metals to mixed silicate surfactant gels prior to the hydrothermal synthesis. We have systematically studied the formation of hexagonal structure of MCM-41 and the formation of rhodium oxide nanoparticles, while changing the temperature, aging time and Si/Rh ratio during the hydrothermal synthesis. We report here the first synthesis and characterization of Rh-MCM-41.

The synthesis<sup>‡</sup> of Rh-MCM-41 was achieved by modifying the recently reported procedure.<sup>12</sup> The Si/Rh ratio in the synthesis was varied in the range 200–70, and the hydrothermal synthesis was carried out *via* two different pathways [route A: 373 K for 10 days (Rh-MCM-41-A) and route B: 423 K for 48 h (Rh-MCM-41-B)] to study the formation of rhodium oxide particles and also the MCM-41 framework. Supporting Rh on MCM-41 (Rh-su-MCM-41) by an impregnated method was also conducted§ for comparison with Rh-MCM-41. The powder XRD patterns of the calcined forms of Rh-MCM-41 are shown and indexed in Fig. 1. The  $d_{100}$  spacings and the unit cell parameters ( $a_0$ ) are listed in Table 1. A highly ordered hexagonal structure was identified for the Rh-MCM-41-A, which resembled pure Si-MCM-41 reported in the literature.<sup>1,12</sup> A shift of the  $d_{100}$  peak was noticed for the Rh-MCM-41-B, indicating that the  $a_0$  (5.47–5.71 nm) became larger. The increase in the  $a_0$  implies the promotion of polymerization of the silica precursor by the presence of Rh ions in the gel, and eventually thicker pore walls were produced as compared to the

pure Si-MCM-41 ( $a_0 = 5.00$  nm, pore wall thickness: 1.69 nm) prepared under the similar conditions. The increase of  $a_0$  may be due to a catalytic role of rhodium during the construction of the mesoporous framework at 423 K.

The (114) XRD peak of Rh<sub>2</sub>O<sub>3</sub> at  $2\theta = 34.3^\circ$  was not detected for the Rh-MCM-41-B, indicating that rhodium oxides are highly dispersed and/or amorphous. Rh K-edge EXAFS spectra for Rh-MCM-41-A and Rh-MCM-41-B were measured at 20 K using synchrotron radiation at Photon factory (proposal No. 97G002). The curve fitting analysis using the empirical parameters derived from Rh<sub>2</sub>O<sub>3</sub> (Rh–O 0.211 nm, coordination number six), revealed the Rh–O bond distance at 0.205 nm with the coordination number of 4.3–4.5. Preliminary analysis for the second shell also indicated the presence of Rh–Rh bonds at 0.299 nm for Rh-MCM-41-A and at 0.307 nm for Rh-MCM-41-B, the distance being >0.292 nm for Rh<sub>2</sub>O<sub>3</sub>. Hence the rhodium oxide particles in the Rh-MCM-41 seem to have different structures from Rh<sub>2</sub>O<sub>3</sub>.

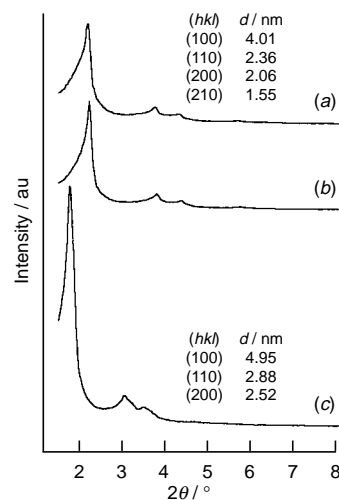


**Fig. 1** Powder X-ray diffraction patterns of the calcined forms of Rh-MCM-41; (a) Rh-MCM-41-A, (Si/Rh = 200); (b) Rh-MCM-41-A(104); (c) Rh-MCM-41-B (200)

**Table 1** Properties of the Rh-MCM-41 molecular sieves

Sample	Si/Rh ratio <sup>a</sup>	$d_{100}$ <sup>b</sup> /nm	$a_0$ <sup>c</sup> /nm	Pore diameter <sup>d</sup> /nm	$S_{\text{BET}}$ /m <sup>2</sup> g <sup>-1</sup>	Pore volume/cm <sup>3</sup> g <sup>-1</sup>	PWT <sup>e</sup> /nm	XPS Si/Rh ratio
Rh-MCM-41-A	200	4.01	4.63	3.02	1016	0.96	1.61	907
Rh-MCM-41-A	70	4.01	4.63	3.02	1028	1.06	1.61	554
Rh-MCM-41-B	200	4.95	5.71	3.40	623	0.80	2.31	415
Rh-MCM-41-B	104	4.74	5.47	3.26	464	0.55	2.21	355
Rh-su-MCM-41	104	4.57	5.27	3.40	1175	0.88	1.87	91

<sup>a</sup> At the synthesis stage. <sup>b</sup> Spacing after calcination. <sup>c</sup> Calculated  $a_0 = 2d_{100}\sqrt{3}$ . <sup>d</sup> Dollimore–Heal method. <sup>e</sup> PWT (pore wall thickness) =  $a_0$  – pore diameter.

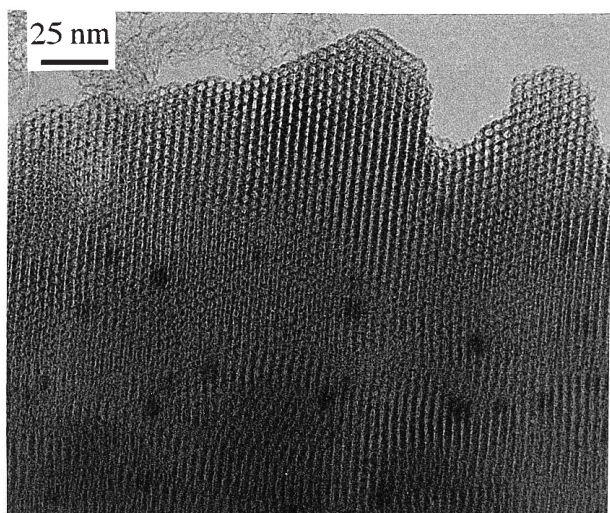


**Fig. 2** TEM micrograph (200 kV;  $\times 80\,000$ ) of the calcined form of Rh-MCM-41-A with Si/Rh ratio of 200

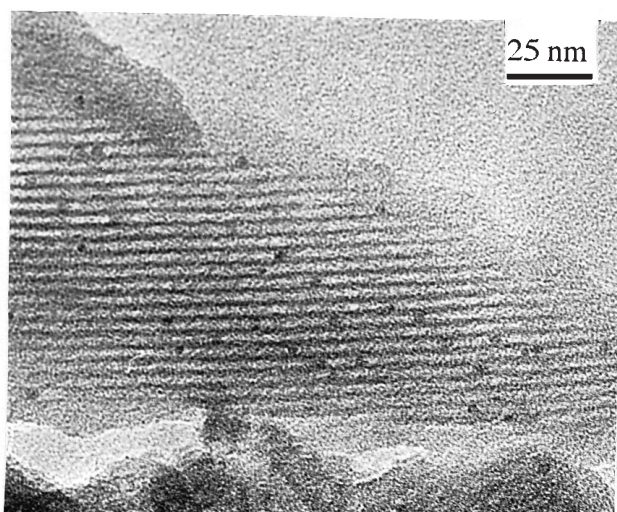


**Fig. 3** TEM micrograph viewed perpendicular to the pore axis (200 kV;  $\times 100\,000$ ) of the calcined form of Rh-MCM-41-B with Si/Rh ratio of 200

The TEM image of calcined Rh-MCM-41-A is shown in Fig. 2, where the hexagonally packed MCM-41 with dispersed rhodium oxide particles with an average particle size of 6 nm is observed. Fig. 3 is the TEM image viewed perpendicular to the pore axis of the calcined Rh-MCM-41-B, which depicts the uniformly packed channels containing dispersed rhodium oxide nanoparticles ( $< 3$  nm), and the  $d_{100}$  value calculated from the TEM image is in agreement with the value from XRD. The thickness of pore walls in TEM is also in agreement with that calculated from XRD in Table 1.

The adsorption-desorption isotherms of  $N_2$  at 77 K were of type IV for Rh-MCM-41 samples which is typical of mesoporous solids and has a narrow pore size distribution. The surface area, pore diameter and pore wall thickness are listed in Table 1. Further characterization of the calcined Rh-MCM-41 samples was performed by  $^{29}\text{Si}$  solid state MAS NMR using cross polarization (CP) technique to examine the formation of thicker pore walls in case of Rh-MCM-41-B. The intensity ratio of the two NMR peaks  $Q^3:Q^4$  for Rh-MCM-41-B was 66:34, while that for pure Si-MCM-41 was 76:24, and this  $Q^3:Q^4$  ratio obtained by CP technique for the Si-MCM-41 is in agreement with that reported by Zhao *et al.*<sup>13</sup> The large increase in the intensity of the  $Q^4$  silicon peak at  $\delta -122$  for Rh-MCM-41-B

indicates the enhancement of cross-linking by rhodium. The  $Q^3:Q^4$  ratio for Rh-MCM-41-A was identical with that for Si-MCM-41.

The location of rhodium oxide particles in Rh-MCM-41 may be deduced by the Si/Rh ratio in XPS spectra. The Si/Rh XPS ratio for Rh-su-MCM-41 with the Si/Rh bulk ratio of 104 was 91, whereas that for Rh-MCM-41-B with the Si/Rh bulk ratio of 104 was 355. All the Rh-MCM-41 samples in Table 1 showed much larger Si/Rh XPS ratios than the values expected from the bulk composition. These results demonstrate that most of rhodium oxide particles in the Rh-MCM-41-A and Rh-MCM-41-B samples are located in the bulk or the mesopore channel, as imaged in Fig. 2 and 3, respectively, whereas rhodium oxides in Rh-su-MCM-41 are thought to be supported at the external surfaces and near the surfaces.

The comprehensive characterization data demonstrate that the growth of nanosized rhodium oxide particles  $< 3$  nm in the mesopore channel of MCM-41 can be controlled with the appropriate selection of synthesis conditions, and that rhodium plays a catalytic role in the polymeric formation of silica walls of the MCM-41 framework. The application of Rh-MCM-41 to catalysis is in progress.

This work has been supported by CREST (Core Research for Evolutionary Science and Technology) of the Japan Science and Technology Corporation (JST). We thank Dr T. Kogure for assistance with some of the TEM observations which were completed in the Electron Microbeam Analysis Facility of the Mineralogical Institute, The University of Tokyo.

## Notes and References

† E-mail: iwasawa@chem.s.u-tokyo.ac.jp

‡ Tetramethylammonium hydroxide pentahydrate (TMAOH) was added to distilled water followed by addition of cetyltrimethylammonium bromide (CTABr) at 303 K.  $\text{RhCl}_3 \cdot 3\text{H}_2\text{O}$  (Wako Chemicals) was added to the solution and stirred for 10 min until the solution became clear, then fumed silica obtained from Sigma was slowly added to the solution. The gel composition was 1.0  $\text{SiO}_2$ :0.19 TMAOH:0.27 CTABr:40  $\text{H}_2\text{O}$ :0.0049–0.14  $\text{RhCl}_3 \cdot 3\text{H}_2\text{O}$ . The gel was aged for 24 h at room temperature and aged at 373 K for 10 days or at 423 K for 48 h. It was filtered, washed with distilled water and dried at 373 K for 12 h, followed by calcination in air at 823 K for 8 h.

§ A methanol solution of  $\text{RhCl}_3 \cdot 3\text{H}_2\text{O}$  was added to the calcined pure Si-MCM-41 and the methanol was evaporated with rotary pump and the resultant solid was dried at 373 K for 12 h, followed by calcination at 823 K for 8 h.

- 1 C. T. Kresge, M. E. Leonowicz, W. J. Roth, J. C. Vartuli and J. C. Beck, *Nature*, 1992, **359**, 710.
- 2 J. S. Beck, J. C. Vartuli, W. J. Roth, M. E. Leonowicz, C. T. Kresge, K. D. Schmitt, C. T.-W. Chu, D. H. Olson, E. W. Sheppard, S. B. McCullen, J. B. Higgins and J. L. Schlenker, *J. Am. Chem. Soc.*, 1992, **114**, 10834.
- 3 X. S. Zhao, G. Q. Lu and G. J. Millar, *Ind. Eng. Chem. Res.*, 1996, **35**, 2075.
- 4 A. Sayari, *Chem. Mater.*, 1996, **8**, 1840.
- 5 A. Corma, *Chem. Rev.*, 1997, **97**, 2373.
- 6 U. Junges, W. Jacobs, I. Voigt-Martin, B. Krutzsch and F. Schüth, *J. Chem. Soc., Chem. Commun.*, 1995, 2283.
- 7 A. Corma, A. Martínez and V. Martínez-Soria, *J. Catal.*, 1997, **169**, 480.
- 8 J. N. Armor, *Appl. Catal. A*, 1994, **112**, N21.
- 9 C. A. Koh, R. Nooney and S. Tahir, *Catal. Lett.*, 1997, **47**, 199.
- 10 C. T. Fishel, R. J. Davis and J. M. Garces, *J. Catal.*, 1996, **163**, 148.
- 11 D. S. Shephard, T. Maschmeyer, B. F. G. Johnson, J. M. Thomas, G. Sankar, D. Ozkaya, W. Zhou, R. D. Oldroyd and R. G. Bell, *Angew. Chem., Int. Ed. Engl.*, 1997, **36**, 2242.
- 12 C. F. Cheng, D. H. Park and J. Klinowski, *J. Chem. Soc., Faraday Trans.*, 1997, **93**, 193.
- 13 X. S. Zhao, G. Q. Lu, A. K. Whittaker, G. J. Millar and H. Y. Zhu, *J. Phys. Chem. B*, 1997, **101**, 6525.

Received in Cambridge, UK, 23rd March 1998; 8/02259C